Bull. Chem. Soc. Jpn. Vol. 79, No. 12, 1963–1976 (2006)

Selected Paper

Ruthenium-Catalyzed Addition of Terminal Alkynes to Alkynylstannanes with Migration of the Stannyl Group

Eiji Shirakawa,*[1] Kouji Nakayama,[2] Ryotaro Morita,[2] Teruhisa Tsuchimoto,[2] Yusuke Kawakami,[2] and Toshiaki Matsubara*[3]

[1]Department of Chemistry, Graduate School of Science, Kyoto University, Sakyo, Kyoto 606-8502

[2]Graduate School of Materials Science, Japan Advanced Institute of Science and Technology, Nomi, Ishikawa 923-1292

[3]Center for Quantum Life Sciences and Graduate School of Science, Hiroshima University, Kagamiyama, Higashi-Hiroshima 739-8530

Received June 8, 2006; E-mail: shirakawa@kuchem.kyoto-u.ac.jp

In the presence of a catalytic amount of a ruthenium complex coordinated with PBu_3, alkynylstannanes ($R^1C{\equiv}CSnBu_3$) were found to accept the addition of terminal alkynes ($R^2C{\equiv}CH$) with a 1,2-shift of the stannyl group to give (*E*)- and (*Z*)-1-tributylstannylbut-1-en-3-ynes ($Bu_3SnC(R^1){=}CHC{\equiv}CR^2$). Various combinations of substrates having an aromatic and/or aliphatic substituent can be used, and the stereochemical outcome depends largely on the character of these substituents. The reaction of aliphatic terminal alkynes proceeds stereoselectively, and substituent R^1 on the alkynylstannanes determines the configuration: *E* for R^1 = alkyl and *Z* for R^1 = aryl. In contrast, the reaction of arylacetylenes gave a mixture of stereoisomers irrespective of the character of substituent R^1 on the alkynylstannane. Ruthenium–β-stannylvinylidene complexes generated from a ruthenium complex and an alkynylstannane with migration of the stannyl group are likely to be key intermediates, which accept addition of the C–H bond of terminal alkynes to give the corresponding stannylenynes. DFT calculation clearly shows that the 1,2-shift of the stannyl group on formation of ruthenium–β-stannylvinylidene complexes is more facile than the corresponding 1,2-hydrogen shift of the coordinating terminal alkynes. The effect of the substituents on the stereoselectivity also is discussed based on the calculation.

Easily accessible alkynylmetals, which by themselves react with various relatively strong electrophiles such as carbonyl compounds and alkyl halides,[1] are known to be effectively activated by transition-metal catalysts to couple with aryl and alkenyl halides.[2] The collaboration between alkynylmetals and transition metals enables us also to conduct the transition metal-catalyzed addition of alkynylmetals to unsaturated hydrocarbons. We have been disclosing the palladium- or nickel-catalyzed carbostannylation[3] of alkynes,[4] 1,3-dienes[5] and 1,2-dienes,[6] which gives synthetically useful alkenyl- and allylstannanes having various conjugated and non-conjugated substituents.[7] On the contrary, unsaturated hydrocarbons are reluctant to add to alkynylmetals probably due to the lack of the method to make alkynylmetals ready to accept addition of unsaturated hydrocarbons. To the best of our knowledge, the addition of unsaturated hydrocarbons to alkynylstannanes has no precedent.

On the other hand, terminal alkynes are known to be activated by ruthenium complexes to form vinylidene complexes,[8] which play important roles in the ruthenium-catalyzed addition to terminal alkynes.[9] The electrophilic α-carbon atom of vinylidene complexes reacts with nucleophiles such as water, amines, alkynes, alkenes, and heteroarenes. Among these, the dimerization of terminal alkynes giving 1,4-disubstituted 1-buten-3-ynes **2** and/or 1,2,3-butatrienes **3** (Scheme 1) is one of the most extensively studied reactions,[10] the mechanism of which has been elucidated both experimentally[10b,c,e] and theoretically,[10e] and the proposed catalytic cycle shown in

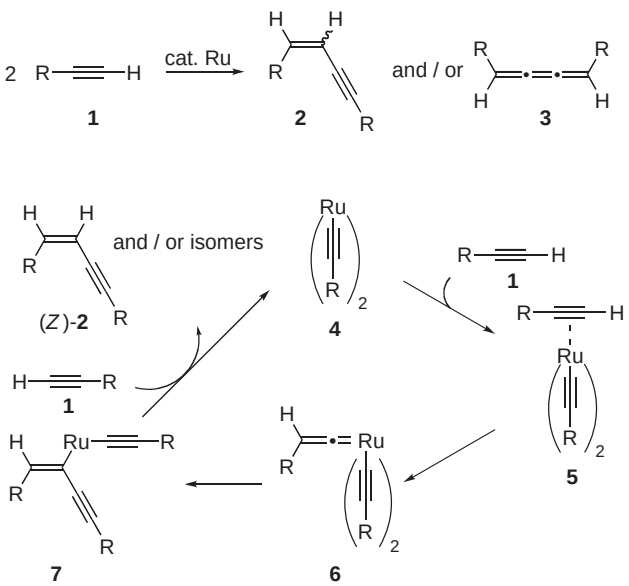

Scheme 1. Ruthenium-catalyzed dimerization of terminal alkynes.

Scheme 1. Terminal alkyne **1** coordinates to bis(alkynyl)ruthenium(II) complex **4** to form ruthenium–alkyne complex **5**, of which the terminal methyne proton undergoes 1,2-migration to give vinylidene complex **6**. One of the alkynyl groups of **6** shifts from the ruthenium atom to the electrophilic α-carbon

Published on the web December 13, 2006; doi:10.1246/bcsj.79.1963

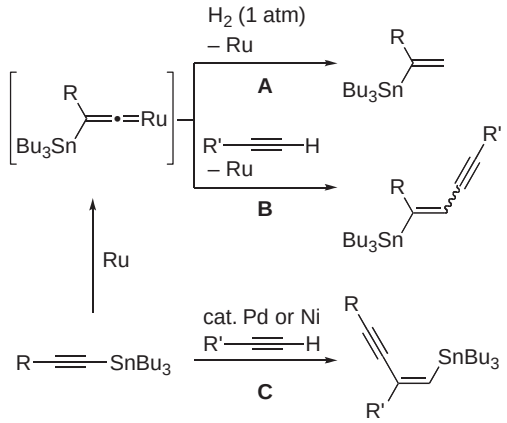

Scheme 2. Addition reactions concerning alkynylstannanes.

atom, giving alkenylruthenium **7**. Finally, dimerization products **2** and/or **3** are generated through the reaction of **7** with another molecule of **1**.

In addition to terminal alkynes, alkynylsilanes are known to form ruthenium–vinylidene complexes, which have been isolated and characterized by X-ray analysis.[11,12] A β-silylvinylidene complex is considered to be a key intermediate in the cyclocarbonylation of 1,1′-bis(silylethynyl)ferrocene, where one of the silyl groups undergoes 1,2-migration.[13,14] We have reported the migration of the metal moiety in the ruthenium-catalyzed hydrogenation of alkynylstannanes (Scheme 2, A).[15,16] Although we have not clarified the mechanism of the hydrogenation, we assumed that the migration of stannyl groups gives ruthenium–β-stannylvinylidene complexes,[17,18] which accept the addition of an hydrogen molecule. Consequently, we anticipated that the β-stannylvinylidene complexes would act like the ruthenium–vinylidene complexes in the ruthenium-catalyzed dimerization of terminal alkynes by accepting the addition of a terminal alkyne, and this turned out to be the case. Here, we report the addition of terminal alkynes to alkynylstannanes with migration of the stannyl group to give 1-stannyl-1-en-3-yne (Scheme 2, B), where the substrates play opposite roles to each other compared to the alkynylstannylation of alkynes (Scheme 2, C). We also report quantum mechanical calculations to clarify the reaction mechanism and determined the activation barrier.

Results and Discussion

Optimization of the Reaction Conditions. We first examined the reaction of tributyl(1-octynyl)tin (**8a**) with phenylacetylene (**9a**). Treatment of **8a** and **9a** with 0.025 molar amount of [di-μ-chlorobis{chloro(*p*-cymene)ruthenium(II)}] ([{RuCl(η^6-*p*-cymene)}$_2$(μ-Cl)$_2$]) and 0.30 molar amount of tributylphosphine (PBu_3) in DMSO at 50 °C for 5 h gave a 67:33 mixture of (*E*)-1-phenyl-4-(tributylstannyl)dec-3-en-1-yne (**10a**) and (*Z*)-isomer **11a** in 90% yield estimated by ^{119}Sn NMR (Entry 1 of Table 1).[19] Dimerization product of **9a** was not detected, showing that the alkyne prefers the alkynylstannane over another molecule of the alkyne as a coupling partner.[20] The results using different solvents are summarized in Table 1. For aprotic solvents, the reaction rate as well as the combined yield of **10a** and **11a** decreases as the polarity of the solvent decreases. Thus, use of DMF instead of DMSO slightly

Table 1. Ruthenium-Catalyzed Addition of Phenylacetylene to Tributyl(1-octynyl)tin: Effect of Solvents[a)]

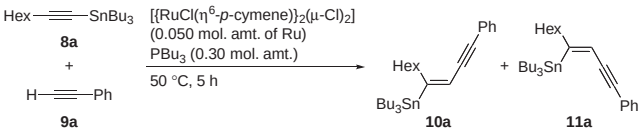

Entry	Solvent	Conversion /%[b)]	Yield /%[b)]	**10a**/**11a**[b)]
1	DMSO	>99	90	67/33
2	DMF	97	76	68/32
3	DMA	24	15	67/33
4	NMP	17	12	67/33
5	THF	18	9	67/33
6	Toluene	15	<1	—
7	EtOH	13	3	>99/1
8	H_2O	5	<1	—
9	DMSO–H_2O (3:1)	88	64	67/33

a) The reaction was carried out in a solvent (0.30 mL) at 50 °C for 5 h using tributyl(1-octynyl)tin (0.40 mmol), phenylacetylene (0.60 mmol), [{RuCl(η^6-*p*-cymene)}$_2$(μ-Cl)$_2$] (0.050 mol amt. of Ru), and PBu_3 (0.30 mol amt.). b) Determined by ^{119}Sn NMR.

lowered the conversion and the yield after 5 h (Entry 2), whereas other amides such as *N*,*N*-dimethylacetamide (DMA) and *N*-methylpyrolidinone (NMP) were much less effective (Entries 3 and 4). Efficiency of THF, one of the most polar ethers, was comparable to NMP, and toluene was totally ineffective (Entries 5 and 6). On the contrary, protic solvents such as ethanol and water were less effective in spite of their high polarity (Entries 7 and 8). It is possible that the insolubility of the substrates as well as the catalyst in water made it ineffective, then we examined a mixed solvent consisting of DMSO–H_2O in a ratio of 3 to 1. The reaction mixture was homogeneous; however, the yield was ever less (Entry 9). We ascribe the high efficiency of DMSO to its ability to coordinate to the ruthenium and/or tin atoms. Considering the steric effect on coordinating ability, the fact that DMF was a better solvent than more bulky DMA and NMP is understandable. In any case, the ratio of stereoisomers **10a** and **11a** was essentially constant.

Next, we examined the effect of ruthenium precursors in the reaction of **8a** with **9a** using DMSO as the solvent (Table 2). In addition to the *p*-cymene complex, the corresponding benzene complex [{RuCl(η^6-C_6H_6)}$_2$(μ-Cl)$_2$] gave a comparable reaction rate and product yield (Entries 1 and 2). Use of $RuCl_3 \cdot nH_2O$, which is one of the most readily available ruthenium complexes, gave an acceptable yield of **10a** and **11a** (Entry 3). Commercially available [$RuH_2(CO)(PPh_3)_3$], which is the best precursor in combination with PBu_3 for the hydrogenation of aliphatic alkynylstannanes with migration of the stannyl group,[15] was much less active (Entry 4). Triphenylphosphine involved in the precursor might lower the catalytic activity. However, high yields of adducts were obtained in the reaction of 1-octyne (**9b**) with **8a** catalyzed by this complex at a higher temperature (80 °C) with a prolonged reaction time (48 h) (Entries 5 and 6). On the other hand, [{RuCl(η^6-*p*-cymene)}$_2$(μ-Cl)$_2$] gave low yields (Entries 7 and 8). Here, again

Table 2. Ruthenium-Catalyzed Addition of Alkynes to Tributyl(1-octynyl)tin: Effect of Precursors[a)]

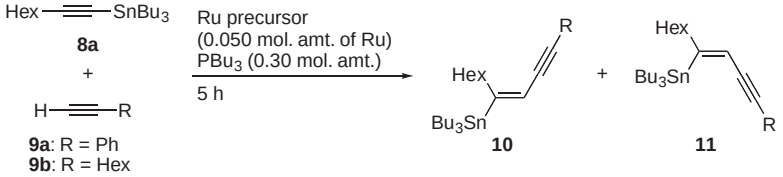

Entry	Alkyne	Ru Precursor	Temp /°C	Conversion /%[b)]	Yield /%[b)]	**10**/**11**[b)]
1	Phenylacetylene (**9a**)	$[\{RuCl(\eta^6\text{-}p\text{-cymene})\}_2(\mu\text{-}Cl)_2]$	50	>99	90	67/33
2	Phenylacetylene (**9a**)	$[\{RuCl(\eta^6\text{-}C_6H_6)\}_2(\mu\text{-}Cl)_2]$	50	98	86	67/33
3	Phenylacetylene (**9a**)	$[RuCl_3 \cdot nH_2O]$	50	99	77	68/32
4	Phenylacetylene (**9a**)	$[RuH_2(CO)(PPh_3)_3]$	50	4	0	—
5	1-Octyne (**9b**)	$[RuH_2(CO)(PPh_3)_3]$	50	2	0	—
6[c)]	1-Octyne (**9b**)	$[RuH_2(CO)(PPh_3)_3]$	80	>99	85	17/83
7	1-Octyne (**9b**)	$[\{RuCl(\eta^6\text{-}p\text{-cymene})\}_2(\mu\text{-}Cl)_2]$	50	86	9	1/>99
8	1-Octyne (**9b**)	$[\{RuCl(\eta^6\text{-}p\text{-cymene})\}_2(\mu\text{-}Cl)_2]$	80	>99	18	1/>99

a) The reaction was carried out in DMSO (0.30 mL) for 5 h using tributyl(1-octynyl)tin (0.40 mmol), an alkyne (0.60 mmol), a ruthenium precursor (0.050 mol amt. of Ru), and PBu_3 (0.30 mol amt.). b) Determined by ^{119}Sn NMR. c) Reaction time = 48 h.

the ratio of **10a** to **11a** was not affected by the precursors, whereas the stereoselectivities in the reaction of **8a** with **9b** changed according to the ruthenium precursors.

In combination with $[\{RuCl(\eta^6\text{-}p\text{-cymene})\}_2(\mu\text{-}Cl)_2]$ as a catalyst precursor, PBu_3 was found to be the most effective ligand among the ligands we examined. Monodentate ligands such as PPh_3, $P(C_6F_5)_3$, $P(c\text{-Hex})_3$, Ph_2PMe, and $PhPMe_2$ as well as bidentate ligands such as $Ph_2P(CH_2)_nPPh_2$ (n = 2–4), $Et_2P(CH_2)_3PEt_2$, and 1,1′-bis(diphenylphosphino)ferrocene gave no adduct, and the conversion was lower than 9% at 50 °C for 5 h. The amount (0.30 mol amt.) of PBu_3 is critical: reduction of the amount lowered the yield considerably and no adduct was obtained without the ligand.

Scope of the Reaction. A ruthenium complex in combination with PBu_3 as a catalyst was applied to the addition reaction between various alkynylstannanes and terminal alkynes (Table 3). $[\{RuCl(\eta^6\text{-}p\text{-cymene})\}_2(\mu\text{-}Cl)_2]$ was found to be effective for most combinations of alkynylstannanes and alkynes, and $[RuH_2(CO)(PPh_3)_3]$ worked well for the reaction between aliphatic substrates. The trimethylstannyl analogue of **8a** underwent the reaction with **9a** in a similar stereoselectivity to **8a** (Entries 1 and 2). Acetylenes having a conjugating aryl or alkenyl group added to **8a**, giving mixtures of stereoisomers (Entries 3–5), whereas the addition of 3,3-dimethyl-1-butyne to **8a** proceeded in a perfect stereoselectivity to give **10e** as the sole product (Entry 6). In contrast, linear terminal alkynes were activated more successfully by $[RuH_2(CO)(PPh_3)_3]$ to add to **8a** in high yields, though the reaction gave a mixture of stereoisomers (Entries 7 and 8). Arylethynylstannanes also accepted the addition of terminal alkynes (Entries 9–13). The reaction between aromatic substrates proceeded in a high stereoselectivity to give **11h** predominantly (Entry 9). 1-Octyne added to phenylethynylstannanes having an electron-donating or -withdrawing group with a perfect stereoselectivity (Entries 11 and 12). A $C(sp^2)$–Br bond, which can be used for further transformation, on a phenylethynylstannane was tolerated (Entry 13). No addition took place with internal alkynes such as 4-octyne and 1-phenyl-1-propyne.

A sequential reaction consisting of the stannylation of a terminal alkyne and the ruthenium-catalyzed addition of the alkyne to the resulting alkynylstannane is also possible. In other words, the stannylative dimerization of terminal alkynes was accomplished by treatment of 1-octyne (**9b**: 0.40 mmol) and Bu_3SnOMe (0.40 mmol) with $[RuH_2(CO)(PPh_3)_3]$ (20 μmol) and PBu_3 (0.12 mmol) in DMSO at 80 °C for 50 h to give an 18:82 mixture of stannylenynes **10f** and **11f** in 69% yield (0.14 mmol) (Eq. 1).

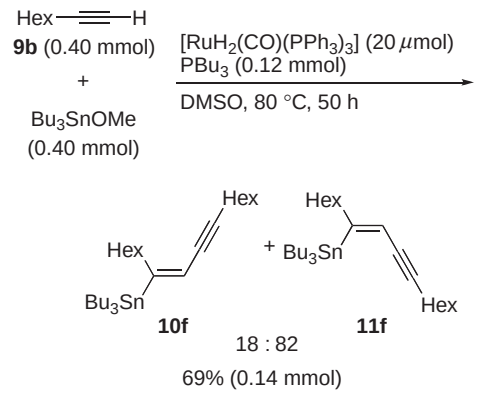

(1)

Application of the Addition Products. These addition products can be transformed to various π-conjugated compounds having an enyne structure. For example, adduct **11i** derived from tributyl(phenylethynyl)tin and 1-octyne was used as a nucleophile and converted into various compounds as shown in Scheme 3. Stannylenyne **11i** coupled with 1-iodo-4-nitrobenzene with an aid of palladium and copper catalysts to give arylenyne **12** in a high yield with retention of the double bond configuration.[7b,c] Alternatively, stannylenyne **11i** was first converted into more nucleophilic lithioenyne **13**, which reacted with electrophiles such as 1-iodobutane and benzaldehyde to give alkylation product **14** and alcohol **15**. Enynol **15** further underwent the palladium-catalyzed cyclization followed by aromatization to give trisubstituted furan **16**.[21]

Reaction Mechanism. Stannyl groups migrate in the pres-

Table 3. Ruthenium-Catalyzed Addition of Terminal Alkynes to Alkynylstannanes[a)]

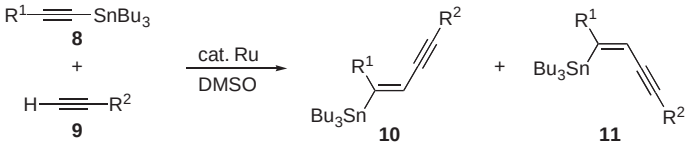

Entry	R^1	R^2	Ru[b)]	Temp /°C	Time /h	Yield /%[c)]	^{119}Sn NMR[d)] Yield/%	**10**/**11**	Product(s)
1	Hex	Ph	A	50	5	85	90	67/33	**10a** **11a**
2[e)]	Hex	Ph	A	40	9	82	85	63/37	**10'a** **11'a**
3	Hex	4-$MeOC_6H_4$	A	50	3	83	88	61/39	**10b** **11b**
4	Hex	4-ClC_6H_4	A	50	25	73	78	57/43	**10c** **11c**
5	Hex	Cyclohexen-1-yl	A	50	8	57	64	63/37	**10d** **11d**
6	Hex	*t*-Bu	A	40	36	62	64	>99/1	**10e**
7	Hex	Hex	B	80	48	83	85	17/83	**10f** **11f**
8	Hex	$CH_3(CH_2)_9$	B	80	48	76	84	17/83	**10g** **11g**
9	Ph	Ph	A	50	7	56	61	4/96	**10h** **11h**
10	Ph	Hex	A	50	9	50	52	1/>99	**11i**
11	4-$MeOC_6H_4$	Hex	A	50	8	55	57	1/>99	**11j**
12	4-$CF_3C_6H_4$	Hex	A	50	20	50	54	1/>99	**11k**
13	4-BrC_6H_4	Hex	A	50	16	54	54	1/>99	**11l**

a) The reaction was carried out in DMSO (0.3 mL) using an alkynylstannane (0.40 mmol), an alkyne (0.60 mmol for Entries 1–5, 7, and 8; 0.80 mmol for Entries 9–13; 2.0 mmol for Entry 6), a ruthenium precursor (Ru = 20 μmol), and tributylphosphine (0.12 mmol). b) A: [{RuCl(η^6-*p*-cymene)}$_2$(μ-Cl)$_2$]; B: [$RuH_2(CO)(PPh_3)_3$]. c) Isolated yield based on the alkynylstannane. d) Determined by ^{119}Sn NMR using tetrabutyltin (tetramethyltin for Entry 2) as an internal standard. e) The trimethylstannyl analogue was used instead of tributyl(1-octynyl)tin (**8a**).

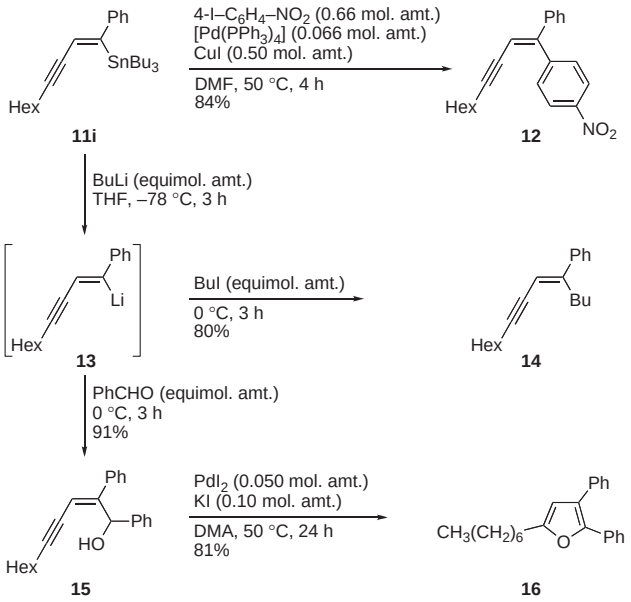

Scheme 3. Transformation of addition product **11i**.

ent reaction in a similar manner to the migration in the hydrogenation of alkynylstannanes.[15] Furthermore, ruthenium complexes have a tendency to form vinylidene complexes Ru=•=C(X)R upon reaction with X–C≡C–R such as terminal alkynes (X = H) and alkynylsilanes (X = $SiMe_3$) with migration of X.[10,11,22] These phenomena convince us that the present reaction proceeds through ruthenium–β-stannylvinylidene complexes, Ru=•=C($SnBu_3$)R, which react with terminal alkynes in the same manner as Ru=•=C(H)R do in the ruthenium-catalyzed dimerization of alkynes. Thus, the only difference between the catalytic cycles of these two ruthenium-catalyzed reactions should be the alkynic substrate transformed to the vinylidene complexes: alkynylstannanes for the present addition vs terminal alkynes for the dimerization. The mechanism of the ruthenium-catalyzed dimerization of terminal alkynes has been elucidated by ab initio molecular orbital analysis,[10e] which shows that the catalytic cycle consists of the formation of vinylidene complex $(RC{\equiv}C)_2Ru{=}\bullet{=}C(H)R$ through coordination of a terminal alkyne on $Ru(C{\equiv}CR)_2$ (Step 1), 1,2-shift of an alkynyl group from Ru to the α-carbon to give RC≡CRuC(C≡CR)=C(H)R (Step 2), and formation of the dimerization product accompanied by regeneration of $Ru(C{\equiv}CR)_2$ (Step 3) (vide supra, Scheme 1).

The entire catalytic cycle of the dimerization of terminal alkynes (Scheme 1) was followed by the density functional method (B3LYP) using the model complex $[Ru(PH_3)_2(C{\equiv}CH)_2]$ and substrate HC≡CH. The energy surface of the catalytic cycle calculated at the B3LYP/BSII//B3LYP/BSII level is displayed in Fig. 1. The catalytic cycle of the dimerization of acetylene mainly consists of Steps 1–3 mentioned above. The geometries of the intermediates and the transition states as well as the feature of the potential energy surface for Step 1 were similar to those calculated previously at the MP2 level for the $[RuCl_2(PH_3)_2]$/HC≡CH system.[10e] Here, it should be noted that the reaction from **5m** to **7m** has a small energy barrier indicating that the migration of the methyne proton of acetylene to the alkenyl carbon is very facile. Intermediate **6m** is quite stable in energy, though the ruthenium atom has a high oxidation state (IV) due to oxidative addition of the acetylene C–H bond. The hydrido in **6m** would migrate as a proton to the alkenyl carbon to form stable C≡C π-coordinate complex **7m**, where the oxidation state of the Ru atom again becomes II. The transition states between **5m** and **6m** as well as between **6m** and **7m** were not determined because the energy surface between **5m** and **7m** is very flat.

We focused on the vinylidene formation (Step 1), which has a large barrier (80.8 kJ mol^{-1}), with acetylene as a starting material and examined Paths A and B shown in Fig. 2 using $Me_3SnC{\equiv}CMe$ instead of acetylene as a substrate. Vinylidene intermediate **3m′** is finally formed in both Paths A and B, where

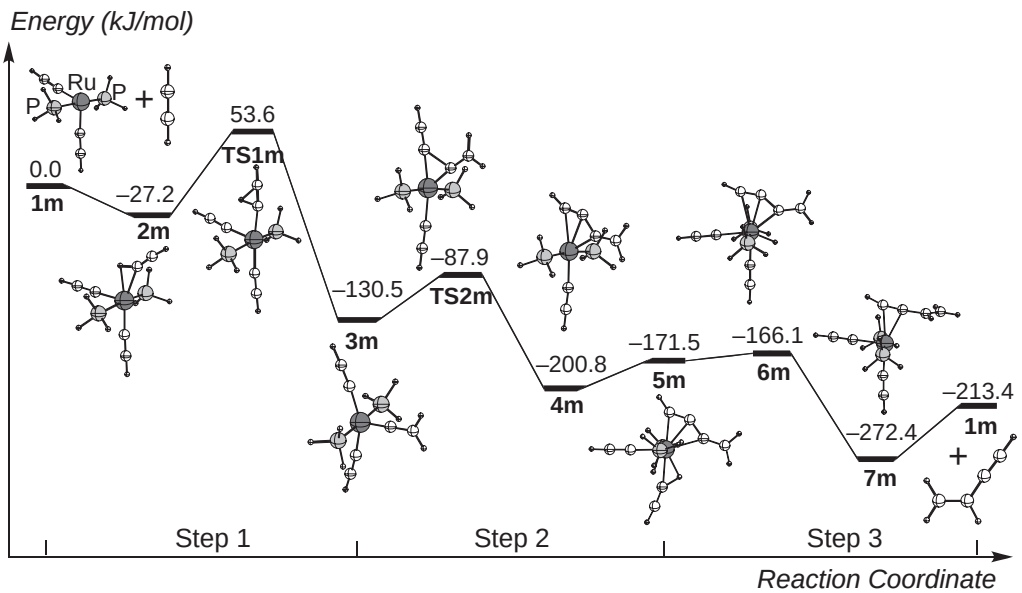

Fig. 1. B3LYP/BSII-optimized equilibrium (**1m**–**7m**) and transition state (**TS1m**–**TS2m**) structures, and the potential energy surface of the full catalytic cycle at the B3LYP/BSII level.

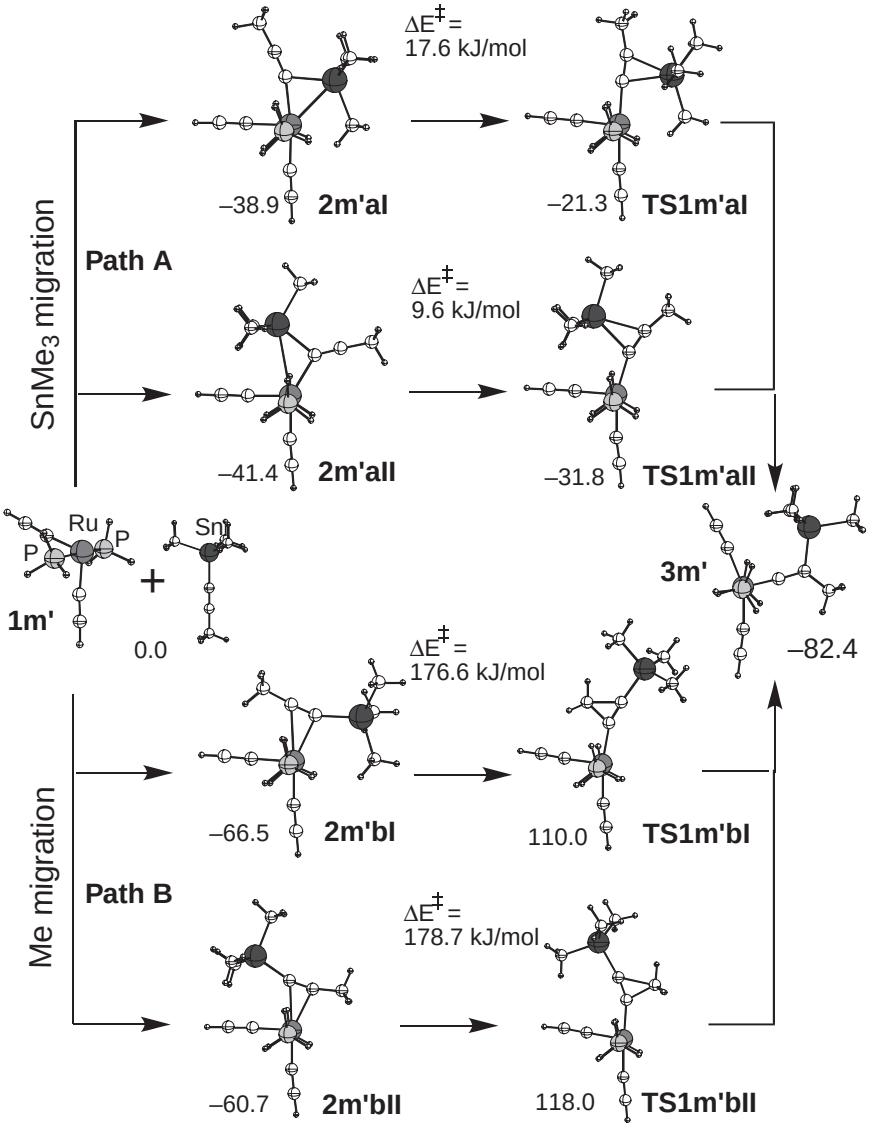

Fig. 2. B3LYP/BSII-optimized equilibrium and transition state structures of Paths A and B with $Me_3SnC{\equiv}CMe$ for Step 1, and their relative energies (kJ mol^{-1}) at the B3LYP/BSII level.

the migrating group is Me_3Sn in Path A and Me in Path B. Each path has two possible directions: the migrating group is far away from ethynyl ligands in a transition state and comes close to the ethynyl ligands in the other transition state. Intermediate **2m′** is Sn–C-σ-complex in Path A while it is C≡C-π-complex in Path B. The energetics of Paths A and B were compared at the B3LYP/BSII level. The energy barriers of Path A are much smaller than those of Path B, which indicates that the former is energetically much more favorable than the latter. This trend is understandable because the positively charged Sn atom[23] of $Me_3SnC{\equiv}CMe$ stabilizes the transition state interacting with the π-electrons of the C≡C bond. The migrating Sn atom also interacts with the π-electrons of the C≡C bond of one of the ethynyl ligands in **TS1m′aII** to further stabilize the transition state. As a result, **TS1m′aII** is 10.5 kJ mol^{-1} more stable than **TS1m′aI**. This also contributes to low energy barrier of 9.6 kJ mol^{-1} for the step from **2m′aII** to **TS1m′aII**, which is 8.0 kJ mol^{-1} smaller than that from **2m′aI** to **TS1m′aI**. Therefore, the large energy barrier (80.8 kJ mol^{-1}) of Step 1 in Fig. 1 would be lowered to 9.6 kJ mol^{-1} by replacement of the terminal methyne proton by a stannyl group, and the catalytic reaction would be controlled in Step 2.

Stereoselectivities in the Addition Reaction. Depending on substituent R^2 on acetylene, the stereochemical outcome in use of [{RuCl(η^6-*p*-cymene)}$_2$(μ-Cl)$_2$] as a catalyst precursor can be divided into two patterns: the addition proceeded stereoselectively for R^2 = alkyl (Types A and B in Scheme 4: Entries 6 and 10–13 of Table 3), whereas mixtures of stereoisomers were produced when R^2 = aryl or alkenyl (Type C in Scheme 4: Entries 1–5 and 9 of Table 3). The reaction proceeded in a perfect selectivity over **10** with Type A, where substrates **8** and **9** which only have alkyl substituents (R^1 and R^2). When we pay attention to the geometric structures involved in the catalytic cycle, we can easily notice that the stereoselectivity of the reaction is determined in the transition state **TS2m** in Step 2, where the stereoselectivity is likely to be governed primarily by steric factors. The catalytic cycles leading to the stereoisomeric products **10** and **11** can be thus

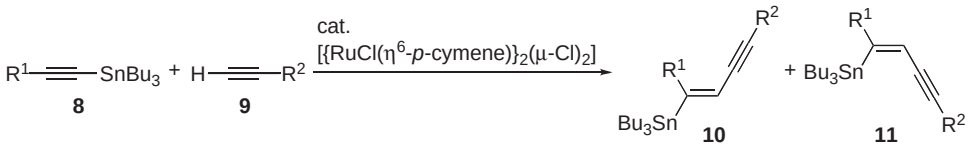

Type	R^1	R^2	
A	alkyl	alkyl	>99/1
B	aryl	alkyl	1/>99
C	alkyl, aryl	aryl, alkenyl	a mixture of stereoisomers

Scheme 4. Stereochemical outcome in use of $[\{RuCl(\eta^6\text{-}p\text{-cymene})\}_2(\mu\text{-}Cl)_2]$ as a catalyst precursor.

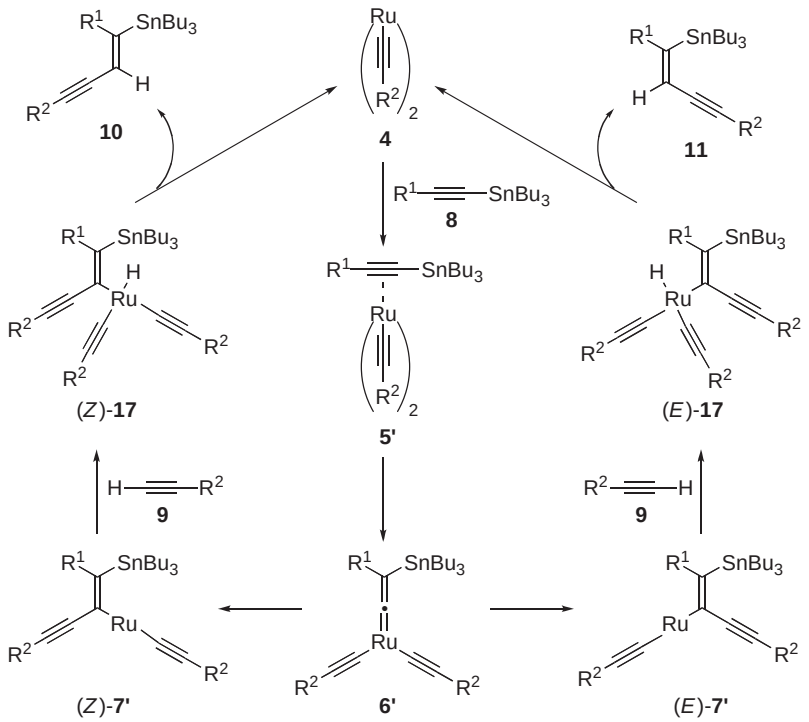

Scheme 5. Possible catalytic cycles of the addition of terminal alkynes to alkynylstannanes.

drawn as shown in Scheme 5. We compared the stability between the transition states that produce the *Z* and *E* products for Types A–C (Fig. 3). A lower energy was found for the transition state that produces (*E*)-product **10** in each case. The calculations showed that the steric contact between the substituents of alkynyl and vinylidene ligands controls the stereoselectivity. The computational results agree with the experimentals for Type A, though there was a discrepancy between the results for Types B and C, suggesting the possibility that the conjugating substituents such as phenyl and alkenyl groups make other factors more important in determining the stereochemistry. The reaction of Type B combination of the substrates proceeds in a stereoselectivity opposite to that with Type A, giving (*Z*)-isomers **11** exclusively. A possible explanation of the stereochemical preference is as follows (Scheme 6 exemplified with $PhC{\equiv}CSnBu_3$). The β-phenyl group derived from $PhC{\equiv}CSnBu_3$ may conjugatedly stabilize transition state **18** leading to (*Z*)-isomers **11**, lying in the plane constructed by the ruthenium atom, the vinylidene moiety and the two alkynyl groups. In contrast, the steric repulsion between the phenyl and the migrating alkynyl groups expels the phenyl ring out of the plane in transition state **19** for (*E*)-isomer **10**, reducing the resonance stabilization. In fact, from calculations (Fig. 4), the energy of transition state **18** is lowest when the dihedral angle ∠C1–C2–C3–C4 is 0°, whereas the phenyl group is largely rotated out of the C3–C4–C5 plane due to steric repulsion in transition state **19** which has a minimum energy when the dihedral angle ∠C1–C2–C3–C4 is 45°. Thus, transition state **18** compared to **19** is likely to be stabilized by the resonance, which is stronger than the steric repulsion between the stannyl and the migrating alkynyl groups.

In contrast to the reaction with Types A and B giving a single isomer, mixtures of stereoisomers were produced in the addition of aryl- and alkenylacetylenes to alkynylstannanes (Type C). From the fact that the reaction of **8a** and **9a**, the combination of which represents Type C, under various conditions gave mixtures of **10a** and **11a** in a constant ratio (67:33), and that use of the trimethylstannyl analogue instead of **8a** hardly affected the selectivity, an equilibrium must be present somewhere in the catalytic cycle. Because, upon the exposure

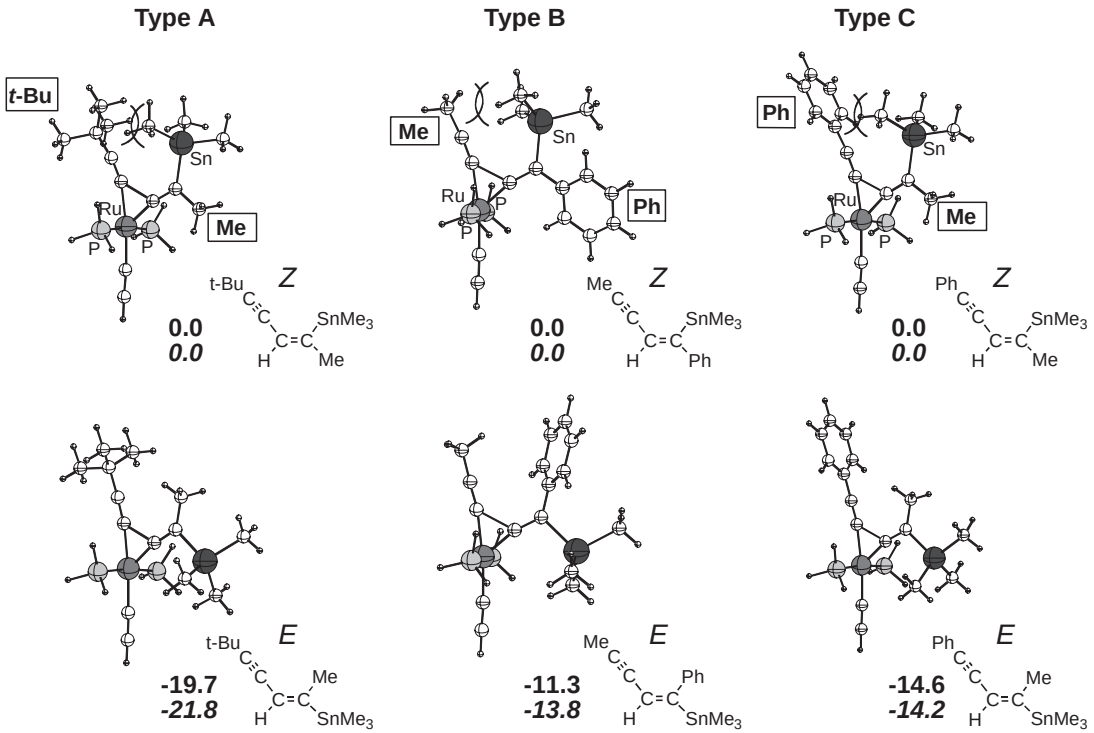

Fig. 3. B3LYP/BSI-optimized structures of the transition states in Step 2 with the various substituents, and their relative energies (kJ mol^{-1}) at the B3LYP/BSI (plain) and B3LYP/BSII (italic) levels. For each case, the *Z* and *E* products are formed through the transition states in the upper and lower sides, respectively.

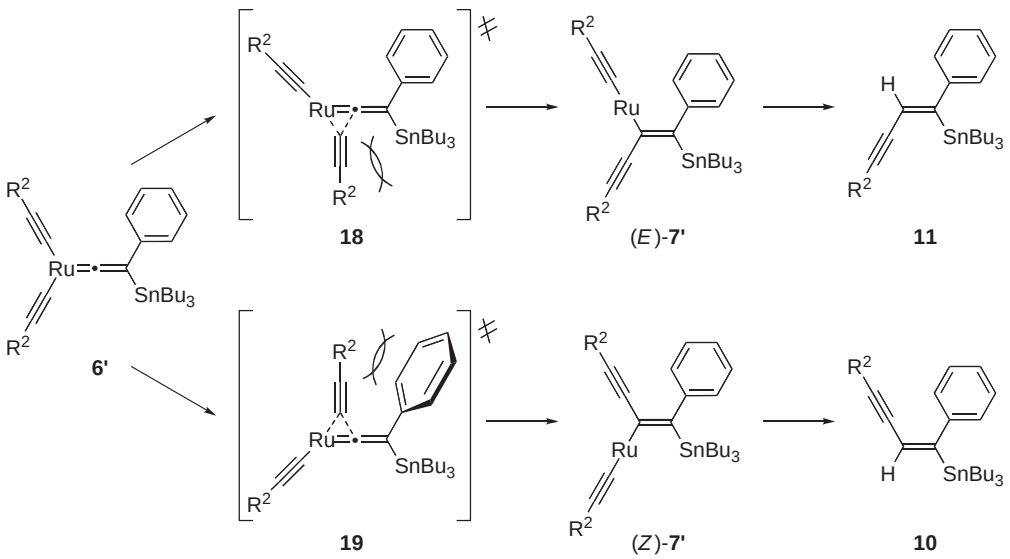

Scheme 6. Stereochemical course with type B combination of substrates.

of **11a** to the reaction mixture of the ruthenium catalyst, **8a** and *p*-methoxyphenylacetylene in DMSO,[24] **11a** did not change and was recovered quantitatively, the equilibrium between addition products **10a** and **11a** can be excluded. Thus, the equilibrium is likely to exist between alkenylruthenium (*Z*)- and (*E*)-**7′** (Scheme 5).[25,26] A possible explanation should be as follows. For the isomerization to take place, the double bond of alkenylruthenium complexes **7′** have to show some single bond character. As shown in Scheme 7 exemplified by the reaction of **8a** with **9a**, the flow of the electrons on the phenyl group into the enyne moiety in (*Z*)- or (*E*)-**7′a** makes the double bond into a single bond to give 1,2,3-butatrienylruthenium **20** or **21**, respectively, which has a carbanion stabilized by the stannyl group.[27] The resulting single bond between the carbon atom coordinated to the ruthenium atom and that attached to the stannyl group rotates to give isomer **21** or **20**, which respectively isomerizes to (*E*)- or (*Z*)-**7′a**.[28] The ruthenium atom may play a role to stabilize the positive charge generated on the benzene ring by donating its own electrons through the triene moiety to form carbene complex **20′**.[29,30]

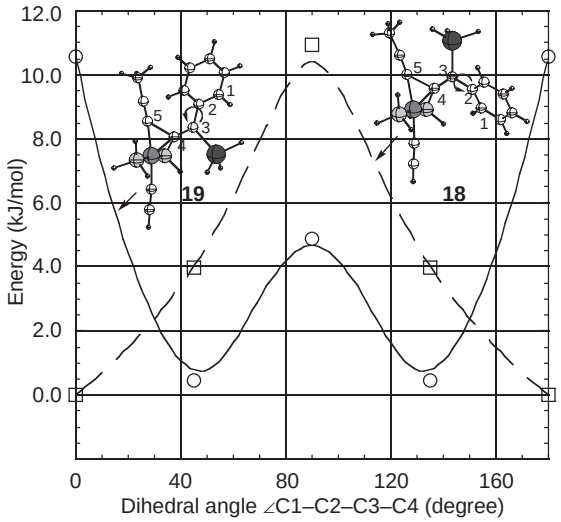

Fig. 4. Energy change of transition state **TS2m** with the Me, Ph, and SnH_3 substituents by the rotation of the Ph substituent around the C2–C3 axis at the B3LYP/BSI level. The geometry at each point was optimized fixing the dihedral angle ∠C1–C2–C3–C4 and the Ru–C4–C5 triangle. ○: The Ph group is on the side of the migrating alkynyl group. □: The Ph group is on the side of the Ru atom.

Conclusion

In conclusion, we have demonstrated that the addition of terminal alkynes to alkynylstannanes with migration of the stannyl group is effectively catalyzed by a ruthenium–PBu_3 complex. The reaction is applicable to various aromatic/aliphatic alkynylstannanes/alkynes, giving (*E*)- and (*Z*)-$Bu_3SnC(R^1)=CHC\equiv CR^2$ with all the substituent patterns, i.e., R^1/R^2 = alkyl/alkyl, alkyl/aryl, aryl/alkyl, and aryl/aryl, which are otherwise hardly accessible even with the palladium- or nickel-catalyzed alkynylstannylation of alkynes giving the same SnC=CC≡C framework. Some examples of synthetic application of the addition products are shown in Scheme 3, though the versatility of this type of stannylenynes has already been demonstrated extensively by transformation of alkynylstannylation products prepared under palladium or nickel catalysis.[7] The reaction mechanism is revealed by the density functional method (B3LYP). The DFT calculation clarified that 1,2-shift of the stannyl group leading to the formation of ruthenium–β-stannylvinylidene complex is facile with energy barrier of only 9.6 kJ mol^{-1}, which is much lower than that (80.8 kJ mol^{-1}) of the 1,2-hydrogen shift in the corresponding ruthenium–terminal alkyne complex. The stereoselectivity is largely affected by substituents on alkynylstannanes (R^1) and terminal alkynes (R^2): (*E*)-stannylenyne for (R^1/R^2 =) alkyl/alkyl; (*Z*)-stannylenyne for aryl/alkyl; a mixture of the stereoisomers for alkyl/aryl and aryl/aryl. The computational results reasonably explain the formation of (*E*)-stannylenyne for combination of R^1/R^2 = alkyl/alkyl, where steric effect compared with electronic effect should be dominant. On the other hand, introduction of conjugating substituents such as phenyl and alkenyl group into the substrates caused some discrepancy between the theoretical and experimental results. However, considering the resonance effect, the stereoselectivity in such cases also should be rationally understood. Not only this new reaction itself should be beneficial for organic synthesis, but also the finding of ruthenium–β-stannylvinylidene complexes will lead to new reactions giving structurally diverse organostannanes.

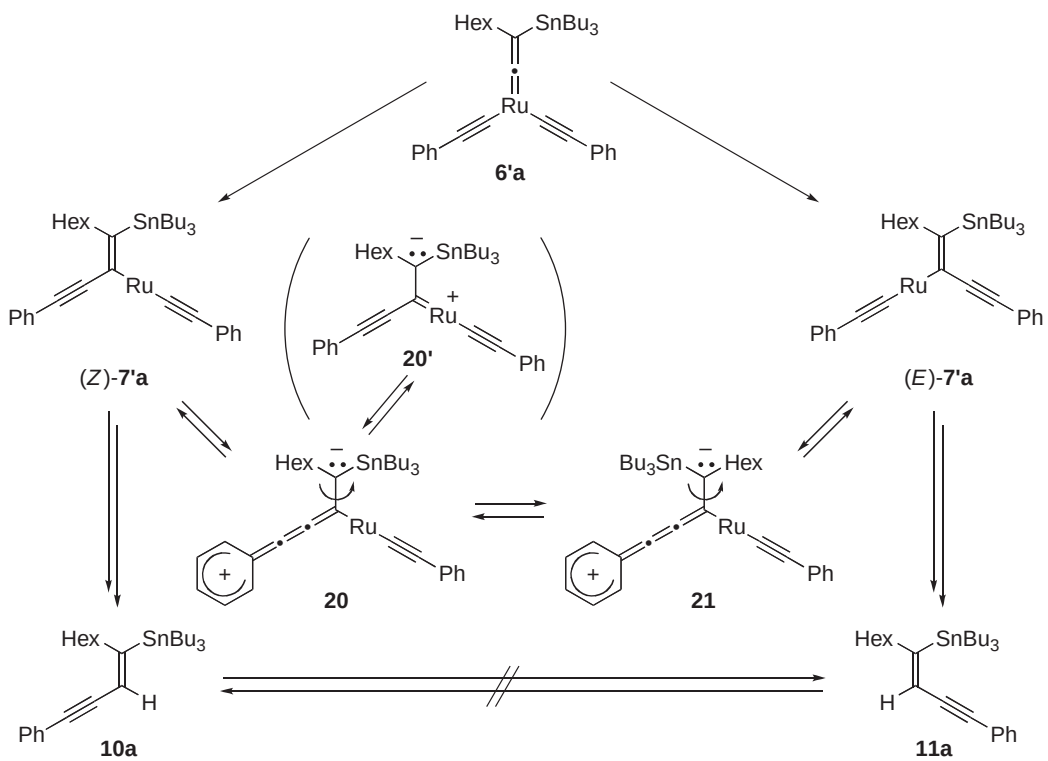

Scheme 7. A possible equilibrium between alkenylruthenium complexes (*Z*)- and (*E*)-**7′a**.

Experimental

General Remarks. All manipulations of oxygen- and moisture-sensitive materials were conducted with a standard Schlenk technique under a nitrogen atmosphere. Nuclear magnetic resonance spectra were taken on a Varian Gemini 2000 (^{1}H, 300 MHz; ^{13}C, 75 MHz) or a Varian UNITY 500 plus (^{13}C, 126 MHz; ^{119}Sn, 186 MHz) spectrometer using tetramethylsilane (^{1}H and ^{13}C) as an internal standard and tetrabutyltin or tetramethyltin (^{119}Sn) as an internal or external standard. The preparative medium-pressure liquid chromatography was performed with YAMAZEN chromatography system equipped with an activated aluminum oxide using hexane as an eluent. Preparative recycling gel permeation chromatography was performed with JAI LC-908 equipped with JAIGEL-1H and -2H using chloroform as an eluent. Elemental analyses were carried out with a Vario EL III machine. High-resolution mass spectra were obtained with a Bruker Bio APEX 70e spectrometer. Unless otherwise noted, reagents were commercially available and used without further purification. Anhydrous DMSO was purchased from Aldrich Chemical Co. and used as received.

Ruthenium-Catalyzed Addition of Terminal Alkynes to Alkynylstannanes with Migration of the Stannyl Group. A General Procedure. An alkyne (0.60, 0.80, or 2.0 mmol) was added to a solution of an alkynylstannane (0.40 mmol), a ruthenium precursor {[{RuCl(η^6-*p*-cymene)}$_2$(μ-Cl)$_2$] (6.1 mg, 0.010 mmol) or [$RuH_2(CO)(PPh_3)_3$] (18.4 mg, 0.0200 mmol)} and tributylphosphine (30 µL, 0.12 mmol) in DMSO (0.30 mL). The mixture was stirred at the temperature specified in Table 3. After the time specified in Table 3, the resulting solution was treated with water (5 mL) and extracted with diethyl ether (20 mL × 3). The combined organic layer was washed with brine (10 mL), and dried over anhydrous magnesium sulfate. Evaporation of the solvent followed by purification with medium-pressure liquid chromatography on aluminum oxide using hexane as an eluent gave stannylenynes **10** and/or **11**. Further separation was performed with recycling gel permeation chromatography, though some of (*E*)-isomers **10** are too unstable to be isolated under the conditions of the chromatography. Consequently, elemental analyses of some products were done as mixtures of **10** and **11** in addition as pure **11**. The results are summarized in Table 3.

(*E*)-1-Phenyl-4-(tributylstannyl)dec-3-en-1-yne (10a): An orange oil, ^{1}H NMR (300 MHz, $CDCl_3$): δ 0.90 (t, J = 7.2 Hz, 12H), 1.05–1.14 (m, 6H), 1.22–1.44 (m, 14H), 1.51–1.65 (m, 6H), 2.51 (td, J = 8.1, 1.2 Hz, 2H), 6.51 (s, 1H), 7.19 (t, J = 7.3 Hz, 1H), 7.31 (t, J = 7.7 Hz, 2H), 7.41 (d, J = 7.4 Hz, 2H). ^{13}C NMR (75 MHz, $CDCl_3$): δ 10.7, 13.5, 14.0, 22.5, 27.3, 28.9, 29.0, 29.5, 31.7, 38.7, 107.9, 127.0, 127.4, 128.5, 134.7, 138.1, 163.0, 167.5. ^{119}Sn{^{1}H} NMR (186 MHz, $CDCl_3$): δ −38.1. Anal. Calcd for $C_{28}H_{46}Sn$: C, 67.08; H, 9.25%. Found as a mixture of **10a** and **11a**: C, 67.19; H, 9.32%.

(*Z*)-1-Phenyl-4-(tributylstannyl)dec-3-en-1-yne (11a): An orange oil, ^{1}H NMR (300 MHz, $CDCl_3$): δ 0.87 (t, J = 7.2 Hz, 12H), 1.05–1.10 (m, 6H), 1.20–1.42 (m, 14H), 1.46–1.64 (m, 6H), 2.32 (t, J = 6.7 Hz, 2H), 6.29 (s, 1H), 7.22–7.36 (m, 3H), 7.37–7.44 (m, 2H). ^{13}C NMR (75 MHz, $CDCl_3$): δ 10.1, 13.6, 14.0, 22.5, 27.3, 28.9, 29.2, 29.7, 31.7, 41.2, 88.3, 90.6, 119.1, 124.0, 127.8, 128.3, 131.3, 165.7. ^{119}Sn{^{1}H} NMR (186 MHz, $CDCl_3$): δ −49.7. HRMS (EI): Calcd for $C_{24}H_{37}Sn$ [M − Bu]$^+$, 445.19154; Found, 445.19290. Anal. Calcd for $C_{28}H_{46}Sn$: C, 67.08; H, 9.25%. Found: C, 66.73; H, 9.29%.

(*E*)-1-Phenyl-4-(trimethylstannyl)dec-3-en-1-yne (10′a): As **10′a** could not be separated from **11′a**, only the NMR data that can be distinguished from the mixture are described. ^{1}H NMR (300 MHz, $CDCl_3$): δ 0.26 (s, 9H), 2.52 (t, J = 7.2 Hz, 2H), 6.50 (s, 1H). ^{119}Sn{^{1}H} NMR (186 MHz, $CDCl_3$): δ −24.7. Anal. Calcd for $C_{19}H_{28}Sn$: C, 60.83; H, 7.52%. Found as a mixture of **10′a** and **11′a**: C, 61.09; H, 7.61%.

(*Z*)-1-Phenyl-4-(trimethylstannyl)dec-3-en-1-yne (11′a): An orange oil, ^{1}H NMR (300 MHz, $CDCl_3$): δ 0.28 (s, 9H), 0.89 (t, J = 6.8 Hz, 3H), 1.20–1.43 (m, 8H), 2.35 (td, J = 7.1, 0.3 Hz, 2H), 6.26 (t, J = 1.5 Hz, 1H), 7.26–7.34 (m, 3H), 7.37–7.43 (m, 2H). ^{13}C NMR (75 MHz, $CDCl_3$): δ −8.8, 14.0, 22.5, 28.8, 29.6, 31.6, 40.7, 88.8, 90.3, 119.0, 123.8, 127.9, 128.4, 131.3, 165.4. ^{119}Sn{^{1}H} NMR (186 MHz, $CDCl_3$): δ −44.5. Anal. Calcd for $C_{19}H_{28}Sn$: C, 60.83; H, 7.52%. Found: C, 60.75; H, 7.63%.

(*E*)-1-(4-Methoxyphenyl)-4-(tributylstannyl)dec-3-en-1-yne (10b): As **10b** could not be separated from **11b**, only the NMR data that can be distinguished from the mixture are described. ^{1}H NMR (300 MHz, $CDCl_3$): δ 2.47 (t, J = 7.7 Hz, 2H), 3.82 (s, 3H), 6.45 (s, 1H). ^{119}Sn{^{1}H} NMR (186 MHz, $CDCl_3$): δ −39.2. Anal. Calcd for $C_{29}H_{48}OSn$: C, 65.55; H, 9.10%. Found as a mixture of **10b** and **11b**: C, 65.41; H, 9.23%.

(*Z*)-1-(4-Methoxyphenyl)-4-(tributylstannyl)dec-3-en-1-yne (11b): A yellow oil, ^{1}H NMR (300 MHz, $CDCl_3$): δ 0.87 (t, J = 7.5 Hz, 12H), 1.00–1.08 (m, 6H), 1.20–1.42 (m, 14H), 1.47–1.60 (m, 6H), 2.31 (t, J = 6.6 Hz, 2H), 3.81 (s, 3H), 6.29 (s, 1H), 6.84 (d, J = 9.0 Hz, 2H), 7.33 (d, J = 9.0 Hz, 2H). ^{13}C NMR (75 MHz, $CDCl_3$): δ 10.1, 13.6, 14.0, 22.5, 27.3, 28.9, 29.2, 29.7, 31.7, 41.1, 55.2, 88.2, 89.2, 114.0, 116.2, 119.3, 132.7, 159.3, 164.5. ^{119}Sn{^{1}H} NMR (186 MHz, $CDCl_3$): δ −50.6. Anal. Calcd for $C_{29}H_{48}OSn$: C, 65.55; H, 9.10%. Found: C, 65.19; H, 9.10%.

(*E*)-1-(4-Chlorophenyl)-4-(tributylstannyl)dec-3-en-1-yne (10c): As **10c** could not be separated from **11c**, only the NMR data that can be distinguished from the mixture are described. ^{1}H NMR (300 MHz, $CDCl_3$): δ 2.50 (t, J = 8.1 Hz, 2H), 6.44 (s, 1H). ^{119}Sn{^{1}H} NMR (186 MHz, $CDCl_3$): δ −38.9. Anal. Calcd for $C_{28}H_{45}ClSn$: C, 62.76; H, 8.47%. Found as a mixture of **10c** and **11c**: C, 62.51; H, 8.50%.

(*Z*)-1-(4-Chlorophenyl)-4-(tributylstannyl)dec-3-en-1-yne (11c): An orange oil, ^{1}H NMR (300 MHz, $CDCl_3$): δ 0.86 (t, J = 7.4 Hz, 12H), 0.99–1.08 (m, 6H), 1.20–1.41 (m, 14H), 1.46–1.60 (m, 6H), 2.32 (t, J = 6.6 Hz, 2H), 6.26 (s, 1H), 7.27 (d, J = 8.7 Hz, 2H), 7.32 (d, J = 8.7 Hz, 2H): ^{13}C NMR (75 MHz, $CDCl_3$) δ 10.1, 13.5, 13.7, 22.5, 27.3, 28.9, 29.1, 29.6, 31.7, 41.2, 87.1, 91.6, 118.8, 122.5, 128.7, 132.5, 133.8, 166.5. ^{119}Sn{^{1}H} NMR (186 MHz, $CDCl_3$): δ −49.9. HRMS (EI): Calcd for $C_{24}H_{36}ClSn$ [M − Bu]$^+$, 479.15257; Found, 479.15397. Anal. Calcd for $C_{28}H_{45}ClSn$: C, 62.76; H, 8.47%. Found: C, 63.06; H, 8.59%.

(*E*)-1-(1-Cyclohexenyl)-4-(tributylstannyl)dec-3-en-1-yne (10d): As **10d** could not be separated from **11d**, only the NMR data that can be distinguished from the mixture are described. ^{1}H NMR (300 MHz, $CDCl_3$): δ 2.40 (t, J = 7.4 Hz, 2H), 5.79–5.86 (m, 1H), 6.19 (s, 1H). ^{119}Sn{^{1}H} NMR (186 MHz, $CDCl_3$): δ −39.2. Anal. Calcd for $C_{28}H_{50}Sn$: C, 66.54; H, 9.97%. Found as a mixture of **10d** and **11d**: C, 66.48; H, 9.96%.

(*Z*)-1-(1-Cyclohexenyl)-4-(tributylstannyl)dec-3-en-1-yne (11d): An orange oil, ^{1}H NMR (300 MHz, $CDCl_3$): δ 0.88 (t, J = 7.2 Hz, 12H), 0.95–1.05 (m, 6H), 1.18–1.40 (m, 14H), 1.44–1.70 (m, 10H), 2.06–2.16 (m, 4H), 2.26 (t, J = 6.5 Hz, 2H), 6.00–6.06 (m, 1H), 6.17 (s, 1H). ^{13}C NMR (75 MHz, $CDCl_3$): δ 10.0, 13.6, 14.0, 21.5, 22.3, 22.5, 25.6, 27.4, 28.8, 29.10, 29.15, 29.7, 31.7, 41.0, 87.8, 90.3, 119.4, 121.1, 134.1, 163.6. ^{119}Sn{^{1}H} NMR (186 MHz, $CDCl_3$): δ −51.3. Anal. Calcd for $C_{28}H_{50}Sn$: C, 66.54;

H, 9.97%. Found: C, 66.53; H, 9.87%.

(*E*)-2,2-Dimethyl-6-(tributylstannyl)dodec-5-en-3-yne (10e): A yellow oil, ^{1}H NMR (300 MHz, $CDCl_3$): δ 0.89 (t, $J = 7.2$ Hz, 12H), 0.95–1.04 (m, 6H), 1.12 (s, 9H), 1.22–1.40 (m, 8H), 1.43–1.60 (m, 12H), 2.37 (td, $J = 7.5$, 1.1 Hz, 2H), 5.66 (s, 1H). ^{13}C NMR (75 MHz, $CDCl_3$): δ 10.3, 13.6, 14.0, 22.5, 27.3, 28.9, 29.5, 29.9, 31.7, 35.3, 38.2, 120.2, 126.2, 162.7, 167.0. ^{119}Sn{^{1}H} NMR (186 MHz, $CDCl_3$): δ −40.3. Anal. Calcd for $C_{26}H_{50}Sn$: C, 64.87; H, 10.47%. Found: C, 64.51; H, 10.37%.

(*E*)-7-(Tributylstannyl)hexadec-7-en-9-yne (10f): An orange oil, ^{1}H NMR (300 MHz, $CDCl_3$): δ 0.76–1.04 (m, 21H), 1.18–1.60 (m, 28H), 2.35 (td, $J = 6.6$, 2.1 Hz, 2H), 2.51 (t, $J = 6.9$, 2H), 5.57–5.63 (m, 1H). ^{13}C NMR (126 MHz, $CDCl_3$): δ 9.8, 13.6, 14.0, 14.1, 19.6, 22.57, 22.64, 27.4, 28.6, 29.0, 29.1, 29.2, 29.7, 31.4, 31.8, 36.6, 78.0, 93.6, 118.3, 162.0. ^{119}Sn{^{1}H} NMR (186 MHz, $CDCl_3$): δ −37.5. Anal. Calcd for $C_{28}H_{54}Sn$: C, 66.01; H, 10.68%. Found: C, 65.88; H, 10.92%.

(*Z*)-7-(Tributylstannyl)hexadec-7-en-9-yne (11f): An orange oil, ^{1}H NMR (300 MHz, $CDCl_3$): δ 0.84–0.93 (m, 15H), 0.94–1.02 (m, 6H), 1.20–1.58 (m, 28H), 2.22 (t, $J = 6.9$ Hz, 2H), 2.28 (td, $J = 6.9$, 2.2 Hz, 2H), 6.02–6.06 (m, 1H). ^{13}C NMR (126 MHz, $CDCl_3$): δ 10.2, 13.7, 14.01, 14.04, 19.7, 22.5, 22.6, 27.5, 28.8, 28.9, 29.0, 29.3, 29.9, 31.4, 31.8, 40.8, 81.4, 89.2, 119.5, 161.9. ^{119}Sn{^{1}H} NMR (186 MHz, $CDCl_3$): δ −50.5. Anal. Calcd for $C_{28}H_{54}Sn$: C, 66.01; H, 10.68%. Found: C, 66.04; H, 10.46%.

(*E*)-7-(Tributylstannyl)icos-7-en-9-yne (10g): An orange oil, ^{1}H NMR (300 MHz, $CDCl_3$): δ 0.82–0.96 (m, 21H), 1.18–1.66 (m, 36H), 2.35 (td, $J = 7.2$, 2.1 Hz, 2H), 2.51 (t, $J = 7.2$ Hz, 2H), 5.57–5.64 (m, 1H). ^{13}C NMR (126 MHz, $CDCl_3$): δ 10.3, 13.8, 14.1, 14.2, 19.8, 22.7, 22.8, 27.6, 29.0, 29.1, 29.2, 29.3, 29.36, 29.42, 29.6, 29.7, 30.0, 31.9, 32.0, 40.9, 78.1, 93.7, 118.3, 162.1. ^{119}Sn{^{1}H} NMR (186 MHz, $CDCl_3$): δ −37.6. Anal. Calcd for $C_{32}H_{62}Sn$: C, 67.96; H, 11.05%. Found: C, 67.91; H, 11.30%.

(*Z*)-7-(Tributylstannyl)icos-7-en-9-yne (11g): An orange oil, ^{1}H NMR (300 MHz, $CDCl_3$): δ 0.84–0.93 (m, 15H), 0.94–1.02 (m, 6H), 1.18–1.58 (m, 36H), 2.22 (t, $J = 7.0$ Hz, 2H), 2.29 (td, $J = 7.0$, 1.8 Hz, 2H), 6.01–6.06 (m, 1H). ^{13}C NMR (126 MHz, $CDCl_3$): δ 10.2, 13.7, 14.0, 14.1, 19.7, 22.6, 22.7, 27.5, 28.9, 29.0, 29.1, 29.2, 29.26, 29.32, 29.5, 29.6, 29.9, 31.8, 31.9, 40.8, 81.4, 89.3, 119.5, 161.8. ^{119}Sn{^{1}H} NMR (186 MHz, $CDCl_3$): δ −50.7. Anal. Calcd for $C_{32}H_{62}Sn$: C, 67.96; H, 11.05%. Found: C, 67.88; H, 10.82%.

(*E*)-1,4-Diphenyl-1-(tributylstannyl)but-1-en-3-yne (10h): A yellow oil, ^{1}H NMR (300 MHz, $CDCl_3$): δ 0.87 (t, $J = 7.2$ Hz, 9H), 0.94–1.02 (m, 6H), 1.29 (sext, $J = 7.3$ Hz, 6H), 1.41–1.58 (m, 6H), 6.08 (s, 1H), 7.18–7.39 (m, 10H). ^{119}Sn{^{1}H} NMR (186 MHz, $CDCl_3$): δ −31.2.

(*Z*)-1,4-Diphenyl-1-(tributylstannyl)but-1-en-3-yne (11h): A yellow oil, ^{1}H NMR (300 MHz, $CDCl_3$): δ 0.83 (t, $J = 7.2$ Hz, 9H), 1.06–1.15 (m, 6H), 1.27 (sext, $J = 7.3$ Hz, 6H), 1.45–1.58 (m, 6H), 6.51 (s, 1H), 7.06–7.14 (m, 2H), 7.17–7.26 (m, 1H), 7.27–7.39 (m, 5H), 7.40–7.53 (m, 2H). ^{13}C NMR (75 MHz, $CDCl_3$): δ 11.0, 13.5, 27.2, 29.0, 90.6, 91.3, 121.5, 123.7, 126.46, 126.53, 128.2, 128.3, 128.4, 131.4, 146.3, 163.1. ^{119}Sn{^{1}H} NMR (186 MHz, $CDCl_3$): δ −43.4. HRMS (EI): Calcd for $C_{24}H_{29}Sn$ [M − Bu]$^+$, 437.12898; Found, 437.12906. Anal. Calcd for $C_{28}H_{38}Sn$: C, 68.17; H, 7.76%. Found: C, 68.05; H, 7.82%.

(*Z*)-1-Phenyl-1-(tributylstannyl)dec-1-en-3-yne (11i): A yellow oil, ^{1}H NMR (300 MHz, $CDCl_3$): δ 0.82–0.94 (m, 12H), 0.99–1.07 (m, 6H), 1.20–1.64 (m, 20H), 2.36 (td, $J = 7.2$, 2.1 Hz, 2H), 6.26 (t, $J = 2.1$ Hz, 1H), 7.00–7.08 (m, 2H), 7.13–7.21 (m, 1H), 7.22–7.32 (m, 2H). ^{13}C NMR (75 MHz, $CDCl_3$): δ 10.8, 13.6, 14.0, 19.7, 22.5, 27.3, 28.6, 28.7, 29.0, 31.4, 81.5, 92.7, 122.1, 126.2, 126.5, 128.2, 146.4, 160.2. ^{119}Sn{^{1}H} NMR (186 MHz, $CDCl_3$): δ −45.4. HRMS (EI): Calcd for $C_{24}H_{37}Sn$ [M − Bu]$^+$, 445.19154; Found, 445.19242. Anal. Calcd for $C_{28}H_{46}Sn$: C, 67.08; H, 9.25%. Found: C, 67.21; H, 9.40%.

(*Z*)-1-(4-Methoxyphenyl)-1-(tributylstannyl)dec-1-en-3-yne (11j): An orange oil, ^{1}H NMR (300 MHz, $CDCl_3$): δ 0.82–0.94 (m, 12H), 0.99–1.07 (m, 6H), 1.22–1.62 (m, 20H), 2.35 (td, $J = 6.9$, 2.4 Hz, 2H), 3.80 (s, 3H), 6.23 (t, $J = 2.4$ Hz, 1H), 6.82 (dt, $J = 8.7$, 2.3 Hz, 2H), 7.00 (dt, $J = 8.7$, 2.3 Hz, 2H). ^{13}C NMR (126 MHz, $CDCl_3$): δ 11.0, 13.6, 14.0, 19.8, 22.6, 27.3, 28.78, 28.81, 29.1, 31.4, 55.3, 81.7, 92.3, 113.7, 121.0, 127.6, 132.7, 139.0, 158.4. ^{119}Sn{^{1}H} NMR (186 MHz, $CDCl_3$): δ −44.9. Anal. Calcd for $C_{29}H_{48}OSn$: C, 65.55; H, 9.10%. Found: C, 65.57; H, 9.01%.

(*Z*)-1-(Tributylstannyl)-1-[4-(trifluoromethyl)phenyl]dec-1-en-3-yne (11k): An orange oil, ^{1}H NMR (300 MHz, $CDCl_3$): δ 0.80–0.96 (m, 12H), 1.08–1.17 (m, 6H), 1.18–1.64 (m, 20H), 2.37 (td, $J = 7.2$, 2.1 Hz, 2H), 6.27 (t, $J = 2.1$ Hz, 1H), 7.12 (d, $J = 8.4$ Hz, 2H), 7.52 (d, $J = 8.4$ Hz, 2H). ^{13}C NMR (126 MHz, $CDCl_3$): δ 11.0, 13.6, 14.0, 19.8, 22.6, 27.3, 28.7, 28.8, 29.1, 31.4, 81.3, 93.8, 123.6, 124.4 (q, $^1J_{C-F} = 271$ Hz), 125.1 (q, $^3J_{C-F} = 3.9$ Hz), 126.6, 128.2 (q, $^2J_{C-F} = 32.7$ Hz), 150.3, 158.8. ^{119}Sn{^{1}H} NMR (186 MHz, $CDCl_3$): δ −41.6. Anal. Calcd for $C_{28}H_{45}F_3Sn$: C, 61.17; H, 7.97%. Found: C, 61.08; H, 7.99%.

(*Z*)-1-(4-Bromophenyl)-1-(tributylstannyl)dec-1-en-3-yne (11l): An orange oil, ^{1}H NMR (300 MHz, $CDCl_3$): δ 0.83–0.93 (m, 12H), 0.99–1.07 (m, 6H), 1.20–1.62 (m, 20H), 2.35 (td, $J = 7.2$, 2.1 Hz, 2H), 6.23 (t, $J = 2.1$ Hz, 1H), 6.82 (dt, $J = 8.4$, 4.5 Hz, 2H), 7.39 (dt, $J = 8.4$, 4.5 Hz, 2H). ^{13}C NMR (126 MHz, $CDCl_3$): δ 11.0, 13.6, 14.0, 19.8, 22.5, 27.3, 28.7, 28.8, 29.1, 31.4, 81.4, 93.3, 120.0, 122.7, 128.1, 131.2, 145.4, 158.8. ^{119}Sn{^{1}H} NMR (186 MHz, $CDCl_3$): δ −43.5. Anal. Calcd for $C_{28}H_{45}BrSn$: C, 57.96; H, 7.82%. Found: C, 57.70; H, 8.02%.

The Sequential Reaction Consisting of the Stannylation of 1-Octyne with Tributyltin Methoxide Followed by the Ruthenium-Catalyzed Addition. A solution of 1-octyne (44.1 mg, 0.400 mmol), $RuH_2(CO)(PPh_3)_3$ (18.4 mg, 0.0200 mmol), tributylphosphine (30 μL, 0.12 mmol), and Bu_3SnOMe (128.4 mg, 0.4000 mmol) in DMSO (0.30 mL) was degassed by three freeze–thaw cycles. After the solution was stirred at 80 °C for 50 h, water (10 mL) was added and the resulting mixture was extracted with diethyl ether (20 mL × 3). The combined organic layer was washed with brine (10 mL), and dried over anhydrous magnesium sulfate. Evaporation of the solvent followed by purification with recycling gel permeation chromatography gave an 18:82 ratio of **10f** and **11f** (70.4 mg, 69%) as a pale yellow oil.

The Palladium-Catalyzed Coupling Reaction of (*Z*)-1-Phenyl-1-(tributylstannyl)dec-1-en-3-yne (11i) with 1-Iodo-4-nitrobenzene. A solution of **11i** (50.1 mg, 0.0999 mmol), 1-iodo-4-nitrobenzene (37.4 mg, 0.150 mmol), $[Pd(PPh_3)_4]$ (11.6 mg, 0.0100 mmol), and CuI (14.3 mg, 0.0751 mmol) in DMF (1.0 mL) was degassed by three freeze–thaw cycles. After the solution was stirred at 50 °C for 4 h, water (10 mL) was added, and the resulting mixture was extracted with diethyl ether (20 mL × 3). The combined organic layer was washed with brine (10 mL) and dried over anhydrous magnesium sulfate. Evaporation of the solvent followed by purification with recycling gel permeation chromatography gave (*Z*)-1-(4-nitrophenyl)-1-phenyldec-1-en-3-yne (**12**: 28.8 mg, 84%) as a pale yellow oil. ^{1}H NMR (300 MHz, $CDCl_3$): δ 0.87 (t, $J = 6.9$ Hz, 3H), 1.20–1.50 (m, 8H), 2.28 (td, $J = 6.9$, 2.1 Hz, 2H), 6.14 (t, $J = 2.1$ Hz, 1H), 7.30–7.43 (m, 5H), 7.64 (dt, $J = 9.0$,

2.1 Hz, 2H), 8.22 (dt, $J = 9.0$, 2.1 Hz, 2H). ^{13}C NMR (126 MHz, $CDCl_3$): δ 14.0, 19.8, 22.5, 28.4, 28.5, 31.3, 79.1, 97.5, 110.5, 123.1, 123.6, 127.7, 128.5, 128.6, 129.8, 130.9, 140.4, 146.4. HRMS (EI): Calcd for $C_{22}H_{23}NO_2$ $[M]^+$, 333.17275; Found, 333.17335.

Alkylation of (*Z*)-1-Phenyl-1-(tributylstannyl)dec-1-en-3-yne (11i). To a solution of **11i** (50.1 mg, 0.0999 mmol) in THF (1.0 mL) was added BuLi (1.58 M in hexane, 63 µL, 0.10 mmol) at −78 °C and the resulting solution was stirred at −78 °C for 3 h. To this was added 1-iodobutane (18.4 mg, 0.100 mmol), and the solution was stirred at 0 °C for 3 h. Water (5 mL) was added, and the resulting mixture was extracted with diethyl ether (10 mL × 3). The combined organic layer was washed with brine (10 mL) and dried over anhydrous magnesium sulfate. Evaporation of the solvent followed by purification by column chromatography on silica gel (hexane) gave (*Z*)-5-phenyltetradec-5-en-7-yne (**14**: 21.5 mg, 80%) as a pale yellow oil. ^{1}H NMR (300 MHz, $CDCl_3$): δ 0.86–0.94 (m, 6H), 1.22–1.64 (m, 12H), 2.41 (td, $J = 6.9$, 2.1 Hz, 2H), 2.78 (t, $J = 7.5$ Hz, 2H), 5.76 (t, $J = 2.1$ Hz, 1H), 7.24–7.40 (m, 5H). ^{13}C NMR (126 MHz, $CDCl_3$): δ 13.9, 14.0, 19.8, 22.6, 27.2, 28.6, 29.0, 30.6, 31.4, 31.9, 79.0, 95.8, 107.5, 126.0, 127.5, 128.3, 140.8, 152.2. HRMS (EI): Calcd for $C_{20}H_{28}$ $[M]^+$, 268.21896; Found, 268.21949.

Hydroxymethylation of (*Z*)-1-Phenyl-1-(tributylstannyl)-dec-1-en-3-yne (11i). To a solution of **11i** (50.1 mg, 0.0999 mmol) in THF (1.0 mL) was added BuLi (1.58 M in hexane, 63 µL, 0.10 mmol) at −78 °C and the resulting solution was stirred at −78 °C for 3 h. To this was added benzaldehyde (10.6 mg, 0.0999 mmol) and the solution was stirred at 0 °C for 3 h. Water (5 mL) was added, and the resulting mixture was extracted with diethyl ether (10 mL × 3). The combined organic layer was washed with brine (10 mL) and dried over anhydrous magnesium sulfate. Evaporation of the solvent followed by purification by column chromatography on silica gel (hexane:ethyl acetate = 10:1) gave (*Z*)-1,2-diphenylundec-2-en-4-yn-1-ol (**15**: 29.0 mg, 91%) as a pale yellow oil. ^{1}H NMR (300 MHz, $CDCl_3$): δ 0.87 (t, $J =$ 6.9 Hz, 3H), 1.21–1.44 (m, 6H), 1.47–1.60 (m, 2H), 2.38 (td, $J = 6.9$, 2.4 Hz, 2H), 2.58 (d, $J = 6.9$ Hz, 1H), 5.95 (t, $J = 2.4$ Hz, 1H), 6.29 (d, $J = 6.9$ Hz, 1H), 7.20–7.28 (m, 6H), 7.29–7.37 (m, 2H), 7.46–7.52 (m, 2H). ^{13}C NMR (126 MHz, $CDCl_3$): δ 14.0, 19.8, 22.5, 28.60, 28.65, 31.3, 73.8, 77.7, 98.3, 110.5, 125.8, 127.1, 127.5, 128.0, 128.2, 128.3, 138.2, 142.2, 152.8. HRMS (EI): Calcd for $C_{23}H_{26}O$ $[M]^+$, 318.19823; Found, 318.19931.

Cycloisomerization of (*Z*)-1,2-Diphenylundec-2-en-4-yn-1-ol (15). A solution of **15** (31.8 mg, 0.0999 mmol), PdI_2 (1.8 mg, 0.0050 mmol), and KI (1.7 mg, 0.010 mmol) in DMA (1.0 mL) was degassed by three freeze–thaw cycles. After the solution was stirred at 50 °C for 24 h, water (10 mL) was added and the resulting mixture was extracted with diethyl ether (20 mL × 3). The combined organic layer was washed with brine (10 mL) and dried over anhydrous magnesium sulfate. Evaporation of the solvent followed by purification by column chromatography on silica gel (hexane:ethyl acetate = 100:1) gave 2,3-diphenyl-5-heptynylfuran (**16**: 25.8 mg, 81%) as a pale yellow oil. ^{1}H NMR (300 MHz, $CDCl_3$): δ 0.90 (t, $J = 6.8$ Hz, 3H), 1.22–1.48 (m, 8H), 1.73 (quint, $J = 7.5$ Hz, 2H), 2.70 (t, $J = 7.7$ Hz, 2H), 6.16 (s, 1H), 7.16–7.38 (m, 6H), 7.38–7.44 (m, 2H), 7.48–7.54 (m, 2H). ^{13}C NMR (126 MHz, $CDCl_3$): δ 14.1, 22.7, 28.0, 28.1, 29.1, 29.2, 31.8, 109.3, 123.0, 126.0, 126.9, 127.0, 128.3, 128.5, 128.6, 131.6, 134.9, 146.6, 155.8. HRMS (EI): Calcd for $C_{23}H_{26}O$ $[M]^+$, 318.19823; Found, 318.19697.

Determination of Configuration of Addition Products 10 and 11. Hydrolysis of 10 and/or 11. To a solution of **10** and/or **11** (0.15 mmol) in THF (10 mL) was added a 6 M HCl aqueous solution (120 µL, 0.72 mmol), and the mixture was stirred at room temperature for 1 h. The resulting solution was treated with a saturated $NaHCO_3$ aqueous solution (5 mL) and extracted with diethyl ether (10 mL × 3). The organic layer was dried over anhydrous magnesium sulfate, and evaporation of the solvent followed by purification by recycling gel permeation chromatography gave **10″** and/or **11″** as a colorless oil. Yields are listed in Table 4.

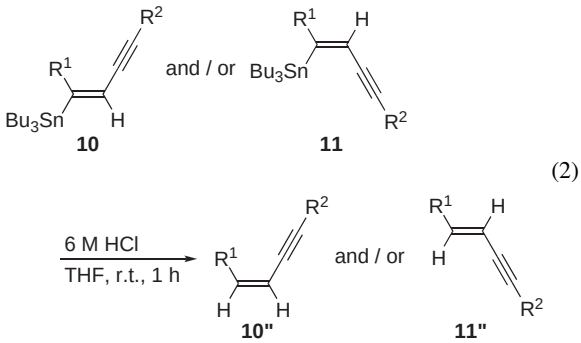

(2)

(*Z*)-1-Phenyldec-3-en-1-yne (10″a): ^{1}H NMR (300 MHz, $CDCl_3$): δ 0.90 (t, $J = 6.9$ Hz, 3H), 1.20–1.60 (m, 8H), 2.32 (tdd, $J = 7.5$, 7.5, 1.5 Hz, 2H), 5.79 (dt, $J = 7.5$, 7.5 Hz, 1H), 6.37 (d, $J = 7.5$ Hz, 1H), 7.20–7.42 (m, 5H).

(*E*)-1-Phenyldec-3-en-1-yne (11″a): ^{1}H NMR (300 MHz, $CDCl_3$): δ 0.90 (t, $J = 6.9$ Hz, 3H), 1.20–1.50 (m, 8H), 2.16 (tdd, $J = 7.2$, 7.2, 1.5 Hz, 2H), 5.69 (dt, $J = 15.9$, 1.5 Hz, 1H), 6.25 (dt, $J = 15.9$, 7.2 Hz, 1H), 7.26–7.44 (m, 5H).

(*Z*)-2,2-Dimethyldodec-5-en-3-yne (10″e): ^{1}H NMR (300 MHz, $CDCl_3$): δ 0.89 (t, $J = 6.8$ Hz, 3H), 1.10 (s, 9H) 1.20–1.55 (m, 8H), 2.20 (dt, $J = 8.7$, 6.0 Hz, 2H), 5.46 (d, $J = 6.8$ Hz, 1H), 5.48 (q, $J = 6.8$ Hz, 1H).

(*E*)-1-Phenyldec-1-en-3-yne (11″i): ^{1}H NMR (300 MHz, $CDCl_3$): δ 0.90 (t, $J = 6.9$ Hz, 3H), 1.25–1.60 (m, 8H), 2.36 (td, $J = 7.5$, 2.4 Hz, 2H), 6.16 (dt, $J = 16.2$, 2.4 Hz, 1H), 6.86 (d, $J = 16.2$ Hz, 1H), 7.26–7.38 (m, 5H).

Table 4 summarizes $^3J_{Sn-H}$ values[31] and chemical shifts (^{119}Sn NMR) of addition products **10** and **11** as well as $^3J_{H-H}$ values of their hydrolyzed products **10″** and **11″**, all of which should contribute the determination of the stereochemistry of the addition reaction.

Computational Details. The density functional calculations were performed by the density functional method using the Gaussian98 program.[32] All the geometry optimizations and energy calculations of the equilibrium and the transition state structures were performed at the B3LYP level[33] using two basis sets, BSI and BSII. LANL2DZ was used for all the atoms, H, C, P, Ru, and Sn in BSI. In BSII, 6-31G** was used for the H, C, and P atoms of the model substrates, HC≡CH and $Me_3SnC{\equiv}CMe$, except for the Me substituents of the $SnMe_3$, and of the model ligand PH_3. For the Me substituents on the $SnMe_3$, 6-31G* was used. For Ru, the triple ζ valence basis functions augmented by an additional single set of f orbitals with the exponents of 1.235,[34] and the effective core potential (ECP) determined by Hay–Wadt[35] to replace the core electrons except for the 16 electrons in the valence shell, and for Sn, the (3s,3p)/[2s,2p] basis functions with a polarization function, i.e., 5d with the exponents of 0.183[36] and the Hay–Wadt ECP[37] to replace the 46 core electrons except for the valence electrons were used. The equilibrium structures and tran-

Table 4. Selected Data of **10**, **11**, and Their Hydrolyzed Products

Entry	R^1	R^2	Product(s)	$^3J_{Sn-H}$ (Hz)		Chemical shift ^{119}Sn NMR (ppm)		Hydrolysis				
									Yield/%		$^3J_{H-H}$/Hz	
				10	**11**	**10**	**11**	Substrate(s)	**10″**	**11″**	**10″**	**11″**
1	Hex	Ph	**10a**, **11a**	20.1	58.1	−38.1	−49.7	**10a** + **11a** (67:33)	78	85	7.4	15.9
								11a		80		15.9
2	Hex	Ph	**10′a**, **11′a**	20.7	60.6	−24.7	−44.5	**10′a** + **11′a** (63:37)	75	86	7.4	15.9
3	Hex	4-MeO-C_6H_4	**10b**, **11b**	20.0	59.1	−39.2	−50.6					
4	Hex	4-Cl-C_6H_4	**10c**, **11c**	19.2	57.1	−38.9	−49.9					
5	Hex	Cyclohexen-1-yl	**10d**, **11d**	21.6	60.3	−39.2	−51.3					
6	Hex	*t*-Bu	**10e**	21.7	—	−40.3	—	**10e**	71		6.8	
7	Hex	Hex	**10f**, **11f**	29.6	60.0	−37.5	−50.5					
8	Hex	$CH_3(CH_2)_9$	**10g**, **11g**	29.4	61.2	−37.6	−50.7					
9	Ph	Ph	**10h**, **11h**	26.1	54.5	−31.2	−43.4					
10	Ph	Hex	**11i**	—	57.3	—	−45.4	**11i**		79		16.2
11	4-MeO-C_6H_4	Hex	**11j**	—	54.8	—	−44.9					
12	4-CF_3-C_6H_4	Hex	**11k**	—	51.5	—	−41.6					
13	4-Br-C_6H_4	Hex	**11l**	—	52.5	—	−43.5					

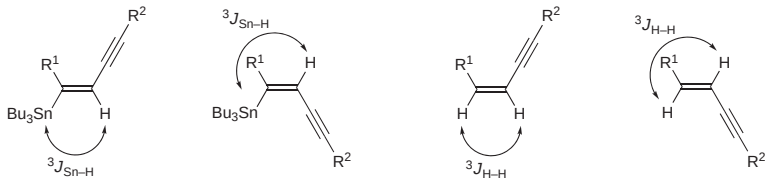

sitions states were fully optimized without any symmetry restrictions and identified by the number of imaginary frequencies calculated from the analytical Hessian matrix. The reaction coordinates were followed from the transition state to the reactant and the product by the intrinsic reaction coordinate (IRC) technique.[38]

We thank Professor Kouichi Ohe (Kyoto University) and Professor Fumitoshi Kakiuchi (Keio University) for helpful discussions. This work has been supported financially by Grant-in-Aids for Scientific Research (No. 17550100) from the Ministry of Education, Culture, Sports, Science and Technology. We thank Daicel Chemical Industries for financial support.

Supporting Information

Cartesian coordinates of computationally optimized structures. This material is available free of charge on the web at http://www.csj.jp/journals/bcsj/.

References

1 L. Brandsma, *Preparative Acetylene Chemistry*, 2nd ed., Elsevier, Amsterdam, **1988**, Chap. 3, pp. 39–77.

2 For recent reviews, see: a) E. Negishi, C. Xu, in *Handbook of Organopalladium Chemistry for Organic Synthesis*, ed. by E. Negishi, Wiley-Interscience, New York, **2002**, pp. 531–549. b) E. Negishi, L. Anastasia, *Chem. Rev.* **2003**, *103*, 1979.

3 For an account of the transition metal-catalyzed carbostannylation of alkynes and dienes, see: E. Shirakawa, T. Hiyama, *Bull. Chem. Soc. Jpn.* **2002**, *75*, 1435.

4 a) E. Shirakawa, H. Yoshida, T. Kurahashi, Y. Nakao, T. Hiyama, *J. Am. Chem. Soc.* **1998**, *120*, 2975. b) E. Shirakawa, H. Yoshida, Y. Nakao, T. Hiyama, *J. Am. Chem. Soc.* **1999**, *121*, 4290. c) E. Shirakawa, K. Yamasaki, H. Yoshida, T. Hiyama, *J. Am. Chem. Soc.* **1999**, *121*, 10221. d) H. Yoshida, E. Shirakawa, T. Kurahashi, Y. Nakao, T. Hiyama, *Organometallics* **2000**, *19*, 5671. e) H. Yoshida, E. Shirakawa, Y. Nakao, Y. Honda, T. Hiyama, *Bull. Chem. Soc. Jpn.* **2001**, *74*, 637.

5 E. Shirakawa, Y. Nakao, H. Yoshida, T. Hiyama, *J. Am. Chem. Soc.* **2000**, *122*, 9030.

6 a) E. Shirakawa, Y. Nakao, T. Tsuchimoto, T. Hiyama, *Chem. Commun.* **2002**, 1962. b) Y. Nakao, E. Shirakawa, T. Tsuchimoto, T. Hiyama, *J. Organomet. Chem.* **2004**, *689*, 3701. Furthermore, the nickel-catalyzed tandem alkynylstannylation of alkynes and 1,2-dienes also has recently been disclosed. c) E. Shirakawa, Y. Yamamoto, Y. Nakao, S. Oda, T. Tsuchimoto, T. Hiyama, *Angew. Chem., Int. Ed.* **2004**, *43*, 3448.

7 For an account of transformation of carbostannylation products of alkynes and 1,2-dienes, see: a) E. Shirakawa, T. Hiyama, *J. Organomet. Chem.* **2002**, *653*, 114. For reviews of the transformation of organostannanes, see: b) V. Farina, V. Krishnamurthy, W. J. Scott, *Org. React.* **1997**, *50*, 1. c) K. Fugami, M. Kosugi, *Top. Curr. Chem.* **2002**, *219*, 87. d) A. G. Davies, *Organotin Chemistry*, 2nd ed., Wiley-VCH, Weinheim, **2004**.

8 For reviews of metal–vinylidene complexes including ruthenium–vinylidene complexes, see: a) M. I. Bruce, *Chem. Rev.* **1991**, *91*, 197. b) C. Bruneau, P. H. Dixneuf, *Acc. Chem. Res.* **1999**, *32*, 311. c) F. E. McDonald, *Chem. Eur. J.* **1999**, *5*, 3103. d) M. C. Puerta, P. Valerga, *Coord. Chem. Rev.* **1999**, *193–195*, 977. e) C. Bruneau, P. H. Dixneuf, *Angew. Chem., Int. Ed.* **2006**, *45*, 2176.

9 For recent reviews on ruthenium-catalyzed reactions, see: a) T. Naota, H. Takaya, S.-I. Murahashi, *Chem. Rev.* **1998**, *98*, 2599. b) B. M. Trost, F. D. Toste, A. B. Pinkerton, *Chem. Rev.* **2001**, *101*, 2067. c) C. Fischmeister, C. Bruneau, P. H. Dixneuf, in *Ruthenium in Organic Synthesis*, ed. by S.-I. Murahashi, Wiley-VCH, Weinheim, **2004**, Chap. 8, pp. 189–217.

10 a) H. Yamazaki, *J. Chem. Soc., Chem. Commun.* **1976**, 841. b) C. Bianchini, M. Peruzzini, F. Zanobini, P. Frediani, A. Albinati, *J. Am. Chem. Soc.* **1991**, *113*, 5453. c) Y. Wakatsuki, H. Yamazaki, N. Kumegawa, T. Satoh, J. Y. Satoh, *J. Am. Chem. Soc.* **1991**, *113*, 9604. d) Y. Wakatsuki, H. Yamazaki, N. Kumegawa, P. S. Johar, *Bull. Chem. Soc. Jpn.* **1993**, *66*, 987. e) Y. Wakatsuki, N. Koga, H. Yamazaki, K. Morokuma, *J. Am. Chem. Soc.* **1994**, *116*, 8105. f) C. S. Yi, N. Liu, *Organometallics* **1996**, *15*, 3968.

11 a) H. Katayama, F. Ozawa, *Organometallics* **1998**, *17*, 5190. b) H. Katayama, C. Wada, K. Taniguchi, F. Ozawa, *Organometallics* **2002**, *21*, 3285.

12 For rhodium–β-silylvinylidene complexes, see: D. Schneider, H. Werner, *Angew. Chem., Int. Ed. Engl.* **1991**, *30*, 700.

13 K. Onitsuka, H. Katayama, K. Sonogashira, F. Ozawa, *J. Chem. Soc., Chem. Commun.* **1995**, 2267.

14 For the rhodium-catalyzed reactions that are considered to proceed through rhodium–β-silylvinylidene complexes, see: a) J. W. Dankwardt, *Tetrahedron Lett.* **2001**, *42*, 5809. b) M. Murakami, M. Ubukata, Y. Ito, *Chem. Lett.* **2002**, 294. c) M. Murakami, S. Hori, *J. Am. Chem. Soc.* **2003**, *125*, 4720. d) T. Miura, H. Murata, K. Kiyota, H. Kusama, N. Iwasawa, *J. Mol. Catal. A: Chem.* **2004**, *213*, 59.

15 E. Shirakawa, R. Morita, T. Tsuchimoto, Y. Kawakami, *J. Am. Chem. Soc.* **2004**, *126*, 13614.

16 Organoboron compounds reportedly add to alkynylmetals including alkynylstannanes with 1,2-migration of the metal moiety. For a review, see: B. Wrackmeyer, *Coord. Chem. Rev.* **1995**, *145*, 125.

17 Rhodium–β-vinylidene complexes are known to be produced by the reaction of $[RhCl(i\text{-}Pr_3P)_2]_n$ with R–C≡C–$SnPh_3$ through 1,2-shift of the stannyl group. M. Baum, N. Mahr, H. Werner, *Chem. Ber.* **1994**, *127*, 1877.

18 Alkynes substituted by a heteroatom such as sulfur and selenium at the terminal carbon undergo 1,2-shift upon reaction with ruthenium complexes to give the corresponding β-heteroatom-substituted vinylidene complexes. For an example of sulfur, see: a) D. C. Miller, R. J. Angelici, *Organometallics* **1990**, *10*, 89. Selenium: b) A. F. Hill, A. G. Hulkes, A. J. P. White, D. J. Williams, *Organometallics* **2000**, *19*, 371.

19 Configuration of **10a** and **11a** was determined by $^3J_{Sn-H}$ value between the tin atom and the olefinic proton of **10a** and **11a** in addition to $^3J_{H-H}$ value between the olefinic protons of the hydrolyzed products of **10a** and **11a**. For details, see Experimental.

20 The reaction of **9a** under the same conditions but in the absence of **8a** gave a mixture of (*E*)- and (*Z*)-1,4-diphenylbut-1-en-3-yne in addition to (*E*)- and (*Z*)-1,4-diphenylbuta-1,2,3-triene (45:45:5:5) in 10% yield.

21 B. Gabriele, G. Salerno, E. Lauria, *J. Org. Chem.* **1999**, *64*, 7687.

22 Alkynyl iodides are known to form tungsten–vinylidene complexes, which undergo electrocyclization. T. Miura, N. Iwasawa, *J. Am. Chem. Soc.* **2002**, *124*, 518.

23 T. Matsubara, K. Hirao, *Organometallics* **2002**, *21*, 4482.

24 The addition of *p*-methoxyphenylacetylene to **8a** took place in a similar manner to Entry 3 of Table 3, giving a 56:44 mixture of **10b** and **11b** in 85% yield.

25 Although alkenylruthenium intermediates **17** in Scheme 5 also should be candidates that are responsible for such an equilibrium, we excluded its participation from the succeeding discussion because of its intrinsic short lifetime suggested by the DFT calculation (Fig. 1, **5m**).

26 As the stereoselectivities should depend not only on the ratio of (*E*)- and (*Z*)-**7′** but also on their reactivities, the result that the ratio of **10a** and **11a** is hardly affected by the ligands, ruthenium precursors and solvents was unexpected.

27 Considering that tin and silicon atoms belong to the same group in the periodic table, trialkylstannyl groups should have the potential to stabilize α-carbanion in a similar manner to trialkylsilyl groups. For an example of the α-carbanion stabilizing ability of silyl groups, see: D. M. Wetzel, J. I. Brauman, *J. Am. Chem. Soc.* **1988**, *110*, 8333.

28 According to the calculation shown in Fig. 1, **7′** should be η^3-butenynyl complexes rather than alkenylruthenium complexes. The ruthenium–η^3-butenynyl structure might contribute to convert the double bond into the single bond. This type of a ruthenium–η^3-butenynyl complex was isolated as an intermediate of the ruthenium-catalyzed dimerization of terminal alkynes and was characterized by X-ray analysis. See Ref. 10b.

29 For an example of the transformation of alkenylruthenium complexes to ruthenium–carbene complexes, see: N. Chatani, H. Inoue, T. Ikeda, S. Murai, *J. Org. Chem.* **2000**, *65*, 4913.

30 In use of $[RuH_2(CO)(PPh_3)_3]$ as a catalyst precursor, mixtures of stereoisomers are obtained even with Type A combination, which lacks a conjugating group on the terminal alkyne (Entries 7 and 8 in Table 3). There is some possibility that the ruthenium complexes generated from this precursor, compared with those derived from $[\{RuCl(\eta^6\text{-}p\text{-cymene})\}_2(\mu\text{-}Cl)_2]$, have stronger tendency to form carbene complexes like **20′**, where the isomerization takes place through the rotation of the C(α)–C(β) single bond.

31 The coupling constant between the tin atom and the *trans*-olefinic proton ($^3J_{Sn-H}$) in alkenylstannanes are reported to be larger than that between *cis*-$^3J_{Sn-H}$. A. J. Leusink, H. S. Budding, J. W. Marsman, *J. Organomet. Chem.* **1967**, *9*, 285.

32 M. J. Frisch, G. W. Trucks, H. B. Schlegel, G. E. Scuseria, M. A. Robb, J. R. Cheeseman, V. G. Zakrzewski, J. A. Montgomery, Jr., R. E. Stratmann, J. C. Burant, S. Dapprich, J. M. Millam, A. D. Daniels, K. N. Kudin, M. C. Strain, O. Farkas, J. Tomasi, V. Barone, M. Cossi, R. Cammi, B. Mennucci, C. Pomelli, C. Adamo, S. Clifford, J. Ochterski, G. A. Petersson, P. Y. Ayala, Q. Cui, K. Morokuma, D. K. Malick, A. D. Rabuck, K. Raghavachari, J. B. Foresman, J. Cioslowski, J. V. Ortiz, B. B. Stefanov, G. Liu, A. Liashenko, P. Piskorz, I. Komaromi, R. Gomperts, R. L. Martin, D. J. Fox, T. Keith, M. A. Al-Laham, C. Y. Peng, A. Nanayakkara, C. Gonzalez, M. Challacombe, P. M. W. Gill, B. G. Johnson, W. Chen, M. W. Wong, J. L. Andres, M. Head-Gordon, E. S. Replogle, J. A. Pople, *Gaussian 98*, Gaussian, Inc., Pittsburgh, PA, **1998**.

33 a) C. Lee, W. Yang, R. G. Parr, *Phys. Rev. B* **1988**, *37*, 785. b) A. D. Becke, *J. Chem. Phys.* **1993**, *98*, 5648.

34 A. W. Ehlers, M. Böhme, S. Dapprich, A. Gobbi, A. Höllwarth, V. Jonas, K. F. Köhler, R. Stegmann, A. Veldkamp, G. Frenking, *Chem. Phys. Lett.* **1993**, *208*, 111.

35 P. J. Hay, W. R. Wadt, *J. Chem. Phys.* **1985**, *82*, 299.

36 S. Huzinaga, *Physical Sciences Data 16, Gaussian Basis Sets for Molecular Calculations*, Elsevier, Amsterdam, **1984**.

37 W. R. Wadt, P. J. Hay, *J. Chem. Phys.* **1985**, *82*, 284.

38 K. Fukui, S. Kato, H. Fujimoto, *J. Am. Chem. Soc.* **1975**, *97*, 1.